Carbohydrate Polymers 92 (2013) 1625–1632

Contents lists available at SciVerse ScienceDirect

Carbohydrate Polymers

journal homepage: www.elsevier.com/locate/carbpol

Starch nanoparticles formation via high power ultrasonication

Sihem Bel Haaj[a], Albert Magnin[b], Christian Pétrier[b], Sami Boufi[a,*]

[a] Laboratoire Sciences des Matériaux et Environnement, LMSE, University of Sfax, BP 802-3018 Sfax, Tunisia
[b] Laboratoire Rhéologie et Procédés, Grenoble-INP, UJF Grenoble 1, UMR CNRS 5520, BP 53, 38041 Grenoble Cedex 9, France

ARTICLE INFO

Article history:
Received 9 September 2012
Received in revised form 22 October 2012
Accepted 1 November 2012
Available online 15 November 2012

Keywords:
Starch
Nanoparticles
Ultrasound

ABSTRACT

Nano-sized starch particles (NSP) were prepared from starch granules using a purely physical method of high-intensity ultrasonication. Particle size distribution, Field Effect Scanning Electron Microscopy (FE-SEM), Raman spectroscopy, and Wide-Angle X-ray Diffraction (WAXD) were used to characterize the morphology and crystal structure of the ensuing nanoparticles. The results revealed that ultrasound treatment of the starch suspension in water and at low temperature for 75 min results in the formation of starch nanoparticles between 30 and 100 nm in size. An attempt to explain the generation of starch nanoparticles was made on the basis of WAXD, Raman analysis and FE-SEM observation. Compared to acid hydrolysis, which is the most commonly adopted process, the present approach has the advantage of being quite rapid, presenting a higher yield and not requiring any chemical treatment.

1. Introduction

The increasing interest in nanomaterials of natural origin and their unique properties have led to intensive research in the area of nano-sized particles from natural polysaccharide polymers such as cellulose (Moon, Martini, Nairn, Simonsen, & Youngblood, 2011), chitin (Zeng, He, Li, & Wang, 2012) and starch (LeCorre, Bras, & Dufresne, 2010). Because of the nanometric size effect, nanoscale fillers typically have greater surface area per mass, leading to higher likelihood self-interaction, which enable mechanical enhancement at lower filler contents than with traditional filler (Siqueira, Bras, & Dufresne, 2010). Furthermore, as the individual components of the nanocomposite are less than one-tenth the wavelength of light, the ensuing nanocomposite is free of scattering, leading to a highly transparent material as long as the polymer matrix is amorphous (Tome et al., 2011).

The extraction of nano-sized particles from natural polysaccharides, namely cellulose, starch and chitin, has been the subject of intense research during the last decade (Dufresne, 2010; Siró & Plackett, 2010; Besbes, Rei Vilar, & Boufi 2011; Alila, Besbes, Rei Vilar, Mutjé, & Boufi, 2013). Materials such as cellulose nanocrystals, microfibrillated cellulose and starch nanocrystals have been extracted from cellulose fibres and starch granules by means of physical or/and chemical treatments.

Although much less studied than nanocellulose or cellulose nanocrystals, the extraction and uses of starch nanocrystals have been the subject of numerous reports (LeCorre et al., 2010; Putaux, Molina-Boisseau, Momaur, & Dufresne, 2003). The potential use of starch nanocrystals as a reinforcing phase in a polymeric matrix and as a barrier agent in packaging materials has been highlighted by several publications (Angellier, Molina-Boisseau, Lebrun, & Dufresne, 2005; Angellier, Putaux, Molina-Boisseau, Dupeyre, & Dufresne, 2005). An interesting review of starch nanoparticle preparation and applications was published by LeCorre et al. (2010).

Starch is a semi-crystalline polysaccharide appearing in nature in the form of granules ranging in size from 1 to 100 μm and is organized in four hierarchical levels (Tester, Karkalas, & Qi, 2004). At the molecular level (~Å), starch is composed of two macromolecular α-1,4-D-glucopyranose units about 5 Å long, namely linear amylose and branched amylopectin; amylopectin is organized in crystalline clusters of double helices forming stacks of alternating crystalline and amorphous lamellae with a regular repeat distance of 9–10 nm, in which the α-1,6-branched branch points reside predominantly in the amorphous lamellae. These are embedded in alternating amorphous and semi-crystalline radial growth rings 100–400 nm thick. The amorphous rings consist of amylose and amylopectin in a disordered conformation, whereas the semi-crystalline rings are formed by the lamellar structure of alternating crystalline and amorphous regions. Given the hierarchical structure of starch, it is possible to extract platelet-like nanoparticles commonly referred to as starch nanocrystals. The main approach adopted to produce starch nanocrystals is based on the use of acid hydrolysis to dissolve the amorphous and paracrystalline regions of the starch granules (Angellier, Molina-Boisseau, et al., 2005; Angellier, Putaux, et al., 2005). The ensuing nanoparticles are parallelepipedic-shaped nanoplatelets around 5–7 nm thick, 20–40 nm long and 15–30 nm wide. However, the main drawbacks of such a method remained the long duration, along with the low yield being in the range of

* Corresponding author. Tel.: +216 74274400; fax: +21674274437.
E-mail address: sami.boufi@fss.rnu.tn (S. Boufi).

0144-8617/$ – see front matter © 2012 Elsevier Ltd. All rights reserved.
http://dx.doi.org/10.1016/j.carbpol.2012.11.022

2–15%, although recent publications report improvements of the yield and reduction of the duration of the treatment (LeCorre, Bras, & Dufresne, 2011; LeCorre, Vahanian, Dufresne, & Bras, 2012).

Not much research has been performed to produce starch nanoparticles using physical treatments. The isolation of NSP using high-pressure homogenization was reported by Liu et al. for the production of starch nanoparticles leading to crystalline microparticles turning into amorphous nanoparticles with increasing run numbers (Liu, Wu, Chen, & Chang, 2009). Chin, Pang, and Tay (2001) reported on starch nanoparticles synthesized by precipitating dissolved starch solution in absolute ethanol under controlled conditions. However, the mean size of the particles remained fairly large (between 200 and 400 nm) and added surfactant during the precipitation process was necessary to obtain particles with size around 200 nm. Another environmentally friendly mechanical approach to producing starch nanoparticles less than 400 nm in size was described in two patents (Giezen et al., 2000; Wildi et al., 2011). The process is based on reactive extrusion of cross-linked plasticized starch followed by grinding and high-speed dispersion in water. A recent publication (Song, Thioc, & Deng, 2011) investigated the mechanism of starch nanoparticle formation via reactive extrusion and analysed the mains parameters governing the particle size.

The effect of ultrasound treatment on the physical properties of starch suspensions has been the subject of numerous reports. Izidoro, Sierakowski, Haminiuk, De Souza, and De Paula Scheer (2011) showed an improvement in starch solubility, swelling power and water absorption capacity after ultrasound treatment (24 W power with 40% amplitude at a frequency of 20 kHz) for 1 h. The same trend was noted by Luo et al. (2008) and Jambrak et al. (2010), who showed that ultrasound treatment results in a decrease in the viscosity consistency index, and enthalpy of gelatinization. They concluded that ultrasound treatment resulted in the distortion of the crystalline region, favouring the swelling power of the treated starch. Biskupa, Rokita, Lotfy, Ulanski, and Rosiak (2005) reported that 360 kHz ultrasound on aqueous solutions of starch at room temperature and for up to 3 h led to a drop in the molecular weight caused by chain scission of starch macromolecules. Gallant, Sterling, Guilbot, and Degrois (1972) and Degrois, Gallant, Baldo, and Guilbot (1974) were the first to report that ultrasound treatment of starch caused physical degradation of the starch granules. Zhu, Li, Chen, and Li (2012) studied the effect of ultrasonic treatment of potato starch granules in excess water on changes in the supramolecular structure. The results showed that ultrasonic treatment (power lower than 155 W) for 30 min at temperatures ranging from 20 to 30 °C affected cluster structure, especially the crystalline region, with a reduction in the molecular order in crystalline lamellae. Surface erosion with notch and groove formation was noted after 30 min ultrasonication at 155 W, but no fragmentation of the starch granules was pointed out, nor any reduction in particle size. Recently, Yue, Zuo, Hébraud, Hemar, and Ashokkumar (2012) studied the impact of ultrasound treatment on potato starch granules in aqueous dispersions at a low temperature around 5 °C. The study showed that treatment of starch granule suspensions by high-intensity low-frequency ultrasound for up to 30 min resulted in damage to the starch surface and in some cases in the shattering of the granules.

From a critical review of the published literature, most studies have focused mainly on changes in the gelatinization and solubility properties of starch following ultrasound treatment. In addition, most ultrasound intensity levels did not exceed 30 min and the sonication treatment was performed at room temperature.

As a contribution to the development of a simple and environment-friendly approach for the preparation of starch-based nanoparticles (SNP), we investigated the isolation and characterization of NSP using high-intensity ultrasonication without any additional chemical treatments and a low temperature of 8–10 °C, in order to prevent plasticization with water and orientate the effect towards maximum particle size reduction.

2. Materials and methods

2.1. Materials

Waxy maize (WaxylisTM, >99% amylopectin) and standard maize starch (70% amylopectin) were provided by Roquette S.A., Lesterm, France.

2.2. Sonication conditions

A 24 kHz Branson digital Sonifier S-450D (Germany) coupled with a horn (tip diameter of 13 mm) was used to treat the starch dispersions. Ultrasonic power dissipated, 170 W, was evaluated using the calorimetry method (Koda, Kimura, Kondo, & Mitone, 2003)

The ultrasonication treatment of the starch suspension was carried as follow; 100 ml of the starch suspension with a solid content of 1.5%, kept in a glass cell, was immersed in a water bath at a constant temperature of 8 ± 1 °C, and sonicated at 80% power output for more than 75 min. Samples of the starch suspension were withdrawn at different intervals for particle size and optical transmittance measurements.

The temperature, not optimized, was selected because at 20 kHz, lower temperature enhances sonochemical activity (Jiang, Pétrier, & Waite, 2006; Mason & Lorimer, 2002), and above 80% power (170 W), it has been seen that the strong cavitation activity increases the coalescence among the bubbles, lowering the efficiency of chemical and physical effects (Mason & Lorimer, 2002).

2.3. Wide-angle X-ray diffraction (WAXD)

Wide-angle X-ray diffraction analysis was performed on powders obtained from both native starch and freeze-dried SNP suspensions. The measurements were performed with a PANanalytical, X'Pert PRO MPD diffractometer equipped with an X'celerator detector. The operating conditions for the refractometer were: Cu Kα radiation, 2θ between 4° and 44°, step size 0.084°, and step time: 250 s.

2.4. Raman spectroscopy

Raman spectra were collected on a LabRAM Analytical Raman micro-spectrograph (Jobin-Yvon, Horiba Group, France) using a He—Ne laser source as exciting radiation ($\lambda = 632.8$ nm) and an air-cooled CDD detector. The samples of starch after ultrasonication were freeze-dried prior to the analysis.

2.5. Transmittance measurements

Starch dispersions at different intervals of ultrasonication were introduced into quartz cuvettes and the transmittance was measured between 400 and 800 nm using a Shimadzu UV–vis spectrophotometer. The samples were not diluted before starting the measurements.

2.6. Particle size determination

The particle diameters were measured at 25 °C using a Malvern Nano-Zetasizer ZS Instrument at a fixed scattering angle of 173°. The dispersions were not diluted before starting the measurements. Dynamic light scattering (DLS) measurements give a *Z*-average size. Each measurement was performed in triplicate and the values averaged to obtain the mean particle size.

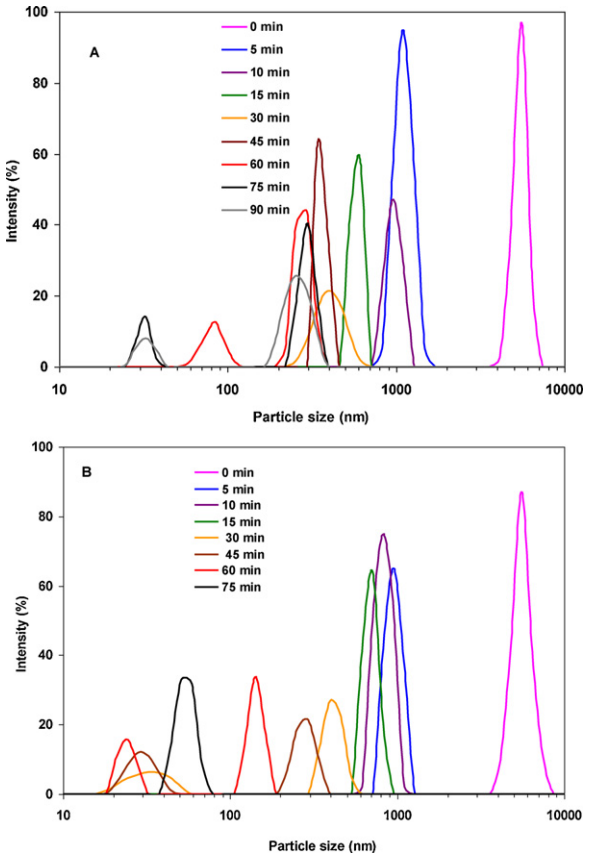

Fig. 1. Change in particle size distribution of the starch suspension: (A) waxy maize and (B) standard maize starch after different ultrasonication times.

2.7. Field-Emission Scanning Electron Microscopy (FE-SEM)

Field Emission Scanning Electron Microscope (FE-SEM) images were obtained with a Zeiss Supra40 fully controlled from a computer workstation. The electron source, a hot cathode producing electrons by Schottky effect, is a tungsten filament coated with a ZrO layer. Images were created by the SMARTSEM software. A drop of a diluted suspension of starch (with a solid content of about 0.02 wt.%) was deposited on a silicon wafer and coated with a thin carbon layer limited to 3 nm applied by sputtering.

3. Results and discussion

3.1. Particle size analysis

The effect of ultrasonication of the starch suspension at a low temperature of 8–10 °C and under high power was analysed by monitoring the change in size distribution during sonication, using starch of two different origins, namely standard starch and waxy maize with high content in amylopectin. As shown in Fig. 1, the particle sizes of both types become smaller as sonication time increases, moving from several μm for the original samples towards about 100–200 nm after 75 min ultrasonication under high power at 24 kHz. It can be seen from the change in particle size vs. sonication time (Fig. 2) that in the case of waxy maize the particle size decreases sharply during the first 30 min, reaching about 500 nm, then continues to decrease more slowly to reach a plateau at about 250 nm after 60 min sonication. Furthermore, it is possible to observe the emergence of particles about 80 nm and 30 nm in size after 60 min and 90 min ultrasonication respectively. The same trend was noted with standard starch up to 45 min.

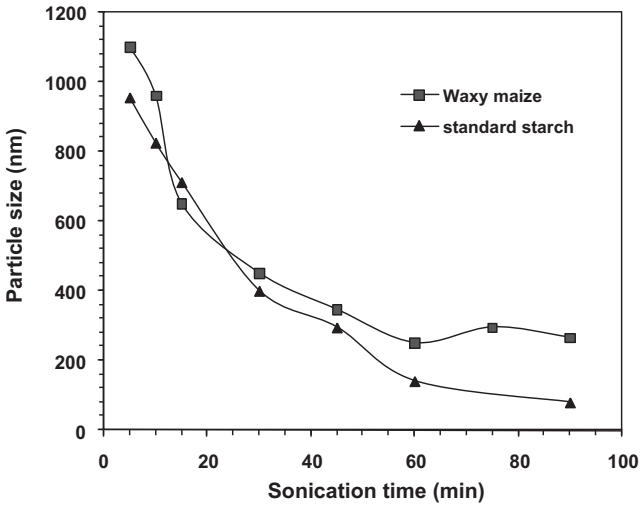

Fig. 2. Change in mean particle size vs. ultrasonication time for waxy maize and standard starch (only particles larger than 100 nm were taken into consideration).

3.2. Optical appearance

The appearance of the starch suspension (at 1.5 wt.% solid content and without any dilution) as a function of the time of ultrasonication is shown in Fig. 3. As the sonication time is augmented, the transparency of the starch suspension improves and the fraction of material settling decreases. After 1 h 15 min utrasonication, the 1.5 wt.% starch slurry became completely transparent without any change in the fluidity of the solution, which is a good indication of the major decrease in size of the starch granule particles. It is also noting that the optical appearance of the dispersion did not change with time and no trace of settling was noted after storing over a period exceeding one month at 8–10 °C.

The transmittance curve from wavelength λ = 400–800 nm is a simple way of obtaining a rough idea of particle size reduction at nanometric scale. Indeed, when light passes through a medium containing randomly dispersed particles, it is scattered by them, causing a reduction in transparency. According to Rayleigh and Mie's law, the scattering loss along the optical pathway is heavily dependent on the relative size of the dispersed phase (d/λ) and the refractive index of the dispersed phase relative to the refractive index of the surrounding medium. Taking into account the mismatch in the refractive index between water (1.31) and that of starch (1.54), the particle size of the dispersed phase will control the transparency of the suspension. Accordingly, for particles of size d less than $\lambda_{min}/10$ (about 40 nm), scattering no longer occurs to any significant extent, resulting in a translucent or even transparent material. Furthermore, Rayleigh scattering prevails in this size range, leading to wavelength-dependence of the transmittance, which is lower at shorter wavelengths.

As shown in Fig. 4, the transmittance degree over the entire visible range increased notably with the ultrasonication time. Interestingly, the change in transmittance degree follows the same trend as the change in particle size, and after 1 h 15 min sonication exceeds 80%, which is a good indication of the absence of micron-sized starch particles.

3.3. Change in morphology

To gain a more accurate idea about the morphology of starch and generated starch particles during the ultrasonication treatment, FE-SEM observations were performed by depositing a drop of diluted starch suspension (with a solid content of about 0.1%) on a silicon wafer.

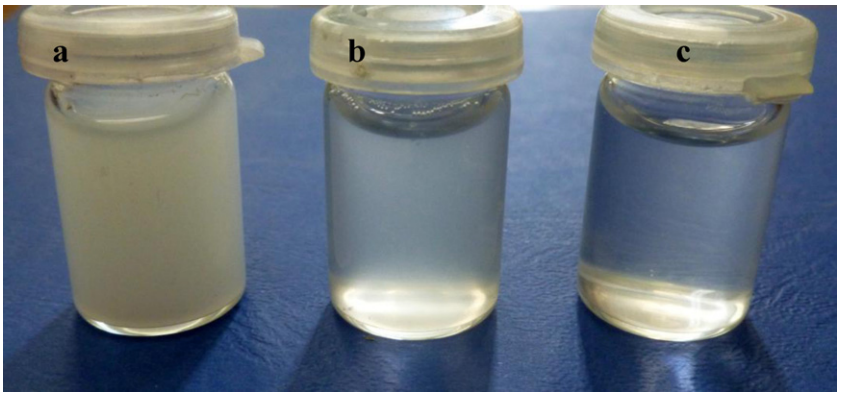

Fig. 3. Appearance of the starch slurry at 1.5 wt.% at different ultrasonication intervals: (a) initial suspension, (b) 45 min and (c) 75 min time after standing for 48 h days at room temperature.

Native waxy starch granules are polygonal with a smooth surface, about 2–15 μm in size with a mean size found to be 17 μm using laser diffraction technique. With increasing ultrasonication time the surface of the granules appears to be progressively broken down and eroded, with the release of nano-sized particles about 20–200 nm in size. This is highlighted in Fig. 5, which shows sample after 45 min ultrasonication. The radial growth rings 200–400 nm thick from which fragments emerged can be clearly seen. Higher magnification of a rising fragment of the eroded surface showed a lamellar structure ranging in thickness from 50 to 80 nm from which the nano-sized particles seem to be detached.

The standard starch particles also have a polyhedral shape and range in size from 2 up to 10 μm. The change in the morphology of standard starch particles during ultrasonication followed the same trend as that of the waxy maize, with seemingly a difference in the appearance of the particles during the erosion process. As ultrasonication progressed, the granule surface changed to rough, displaying the 20–30 nm thick lamellar structure from which nano-sized particles seem to be released.

In both waxy and standard starch, the granular structure of the starch particles was completely loosened after 75 min ultrasonication, giving rise to clusters of particles 80–200 nm in size. The elementary size of the nanoparticles forming the clusters was between 20 and 80 nm. It seems that nanoparticles from waxy maize are less aggregated than those from standard starch. These observations are in agreement with the DLS analysis data, indicating that the particle populations noticed around 20–40 nm in the DLS analysis correspond to individual starch nanoparticles while those observed around 250 nm are aggregated or clustered starch nanoparticles. However, it is difficult to assert from these observations whether the ensuing nanoparticles exhibit platelet or granular morphology.

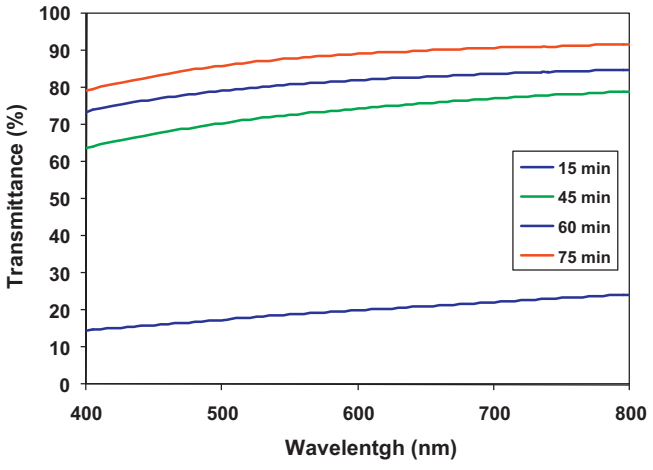

Fig. 4. UV–vis transmittance spectra of the waxy maize slurry at 1 wt.% at different ultrasonication time after standing for 48 h days at room temperature.

Referring to DLS measurement, the initial size of native starch particles were about 6 μm, which is rather low than one revealed from SEM observation being in the range of 5–15 μm. This apparent discrepancy might be rationalized by the specificity of DLS being mainly adapted for sub micron particle. Indeed, DLS measures Brownian motion and relates this to the size of the particles using the Stokes–Einstein equation. Therefore, particles with size more than 10 μm could not be properly detected by DLS as they settle down rapidly. This is the main reason accounting for the rather low particle size of pristine starch granules.

We should also emphasize that FE-SEM observation revealed that no micro-sized particles were observed after 75 min ultrasonication, confirming the complete disintegration of starch granules into nano-sized particles.

3.4. WAXD analysis

X-ray diffraction was used to study the change in starch crystallinity brought about by ultrasound treatment of granular starch. WXAD diffraction patterns of freeze-dried starch samples at different ulrasonication intervals are shown in Fig. 6. As expected, both the standard and waxy maize exhibited the A-type diffraction pattern typical of cereal starch, with the peaks at Bragg angles (2θ) 15°, 17°, 18° and 23° (Zobel, 1964). A small V-type diffraction peak was also observed at 20° for standard starch, which was associated with orderly packed amylose single helical complexes with lipid. An important change in the DRX spectra was noted for both starch types under the effect of ultrasonication. After 30 min ultrasonication all of the diffraction peaks decreased in intensity. With further sonication for 75 min, the diffraction peaks at 10°, 15°, 18° and 23° completely vanished in the case of standard starch, while the peak at 17.5° notably deceased in intensity with the increase in width at half height of the peak. The V-diffraction peak at 20° seems to be unaffected by ultrasonication treatment. However, in the case of waxy maize, all of the diffraction peaks were lost after 75 min sonication and only a broad hallow from 4° to 30° associated with an amorphous phase was observed on the diffraction spectra.

Seemingly, the prolonged ultrasonication of starch granules at a temperature of 8–10 °C and under high ultrasonication resulted in a serious disruption of the crystalline structure of clustered amylopectin, apparently leading to nanoparticles with low crystallinity or an amorphous character. How, though, is it possible to rationalize the decrease or loss of crystallinity under the ultrasonication? Is

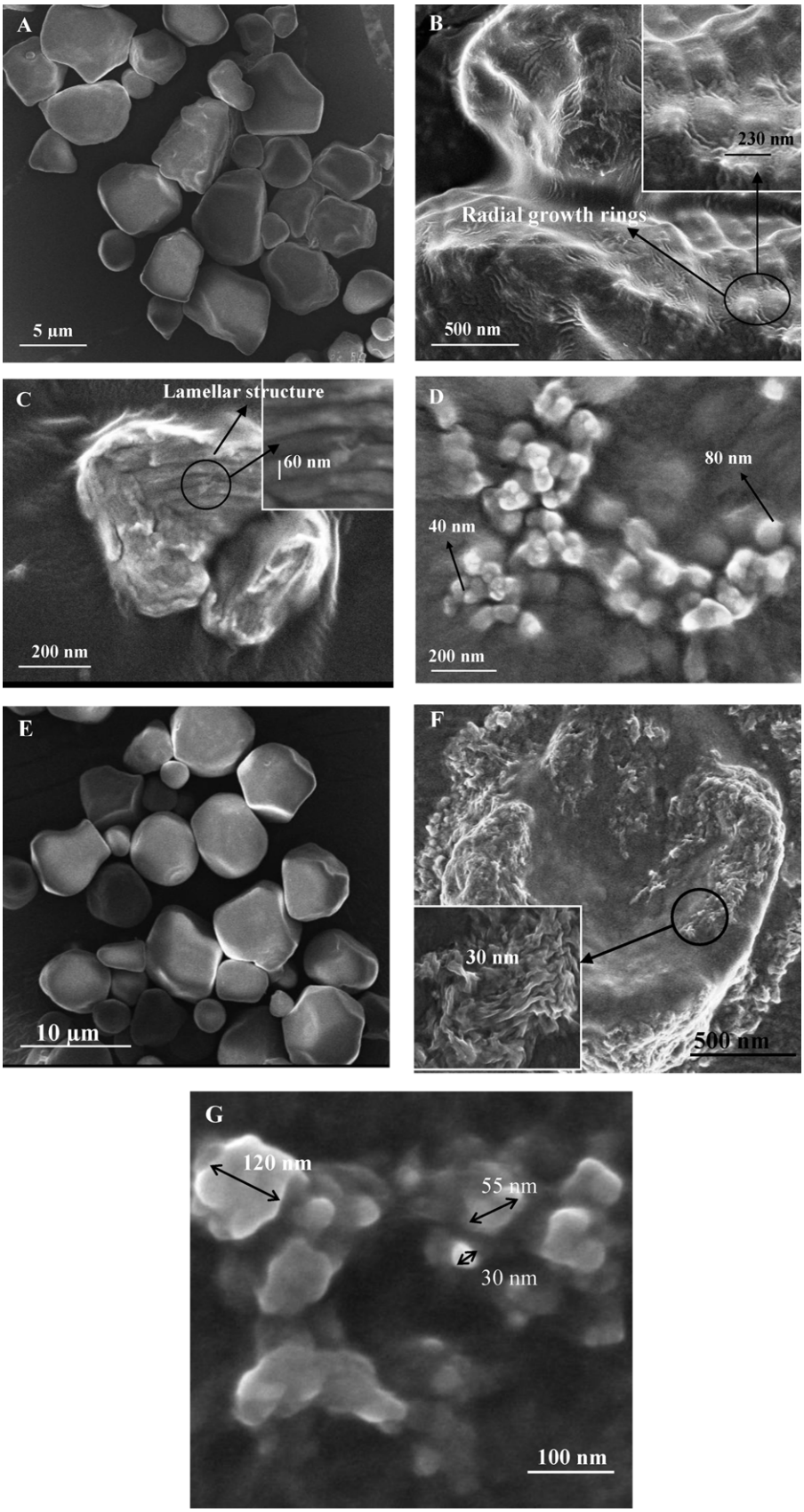

Fig. 5. FE-SEM images of starch particles at different ultrasonication intervals: (A) native waxy maize, (B) waxy maize after 30 min sonication, (C) waxy maize after 45 min sonication, (D) waxy maize after 75 min sonication, (E) native standard maize, (F) standard maize 30 min sonication, and (G) standard maize after 75 min sonication.

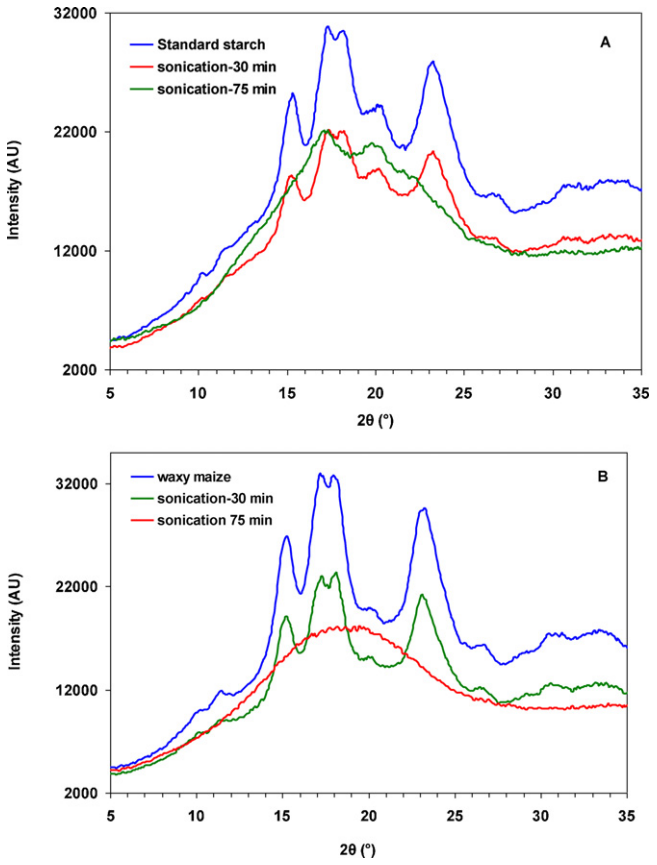

Fig. 6. WXAD diffraction patterns of freeze-dried starch particles: (A) standard maize starch, and (B) waxy maize after different ultrasonication periods.

it not really that the ensuing starch nanoparticles exhibit an amorphous character? In fact, as the particle size decreases down to 20–50 nm, the crystallite size becomes smaller and the diffraction peak becomes broader, since the width at half height of a peak is inversely proportional to the crystallite size. Furthermore, the disappearance of the diffraction peak in the case of waxy maize may be the consequence of the excessive decrease in the crystallite size arising from the reduction in particle size. Indeed, small crystallites that possess only a few lattice planes may not produce sufficiently detectable reflection intensities, especially in the case of light elements such as carbon, in view of the fact that the diffraction is proportional to the square of the atomic number.

3.5. Analysis of structural changes by Raman spectroscopy

FTIR and Raman spectroscopy were used to probe the change in the molecular structure following ultrasonication treatment. The FTIR spectra for starch before and after ultrasonication (spectra not shown) showed almost identical characteristic bands dominated by α-1,4-glycosidic linkage and the C—O—C bond in the glucose ring. For this reason Raman spectroscopy, which is recognized to be more sensitive than FTIR to local changes in polymer microstructure, was carried out. The Raman spectra before and after ultrasonication were recorded and the spectra are shown in Fig. 7. The assignment of the main starch bands, based on data from the literature (Zhbankov, Andrianov, & Marchewka, 1997) is given in Table 1. From this analysis, the following remarks may be made:

- Both the standard starch and waxy maize exhibit the same Raman spectra.

Table 1
Raman wavenumbers and their respective assignment referring to literature data.

Wavenumber (cm^{-1})	Assignment
2910 vs	υ (C—H)
1459 s	δ (CH) + δ (CH_2)
1403 s	δ (C—H)
1381 s	δ (C—H) + δ (CH_2) + δ (C—O—H)
1339 s	δ (C—H)
1260 m	δ (CH_2) + δ (C—O—H) + δ (CH_2—OH)
1126 s	υ (C—O—H) + δ (C—O—H) + υ (C—O)
1081 s	δ (C—O—H)
1050 s	δ (C—O—H) + (C—O—H) + υ (C—C)
941 s	δ (C—O—H) + δ (C—O—C) + υ (C—O)
867 s	υ (C—O—C) + δ (C—H) + δ (CH_2)
763 w	υ (C—C)
711 w	υ (C—C)
614 w	υ (C—C—O)
574 m	υ (C—C—O)
476 vs	υ (C—C—O) + δ (C—C—O)
439 s	δ (C—C—O) + δ (C—C—C)
408 s	υ (C—C—O) + δ (C—C—O)

- The bands due to the skeletal mode vibrations of the glucose pyranose ring of starches exhibit a change after ultrasonication; the bands at 440, 478 and 581 cm^{-1} assigned to ν (C—C—O), δ (C—C—O) and δ (C—C) of pyranose ring skeletal modes respectively undergo a shift of about 5 cm^{-1} towards the higher wavenumber. The bands at 520 and 620 cm^{-1} also assigned to the pyranose ring decrease notably in intensity. Likewise, the bands at 760 and 865 cm^{-1} assigned to ν (C_1—C_2) ring mode and to ν (C_1—O—C_5) respectively undergo a downward shift by about 12 cm^{-1} after sonication treatment. These changes may be related to the decrease in crystallinity following ultrasonication. The same trends in the Raman spectra were noted by Mutungi, Passauer, Onyango, Jaros, and Rohm (2012).
- The vibrations related to the C—O—C of α-1,4 and α-1,6 glycosidic linkages characterized by strong bands in the 900–960 cm^{-1} and a weak band at 1155 cm^{-1} exhibited a change both in intensity and in position. The band at 905 cm^{-1} appearing as a shoulder of the strong band at 940 cm^{-1} seems to vanish after ultrasonication. The band at 940 cm^{-1} is shifted by about 4 cm^{-1} towards the lower wavenumber, and the band at 1155 cm^{-1} decreased in intensity. Considering the band at 905 cm^{-1} associated with α-1,6 glycosidic linkage, it may be inferred that the branching points in the amylopectin were the most affected by ultrasonication, leading to breakage of part of this linkage.
- The band at 1128 cm^{-1} attributed to C—O stretching and C—O—H deformation decrease in intensity after ultrasonication.

The change observed in the Raman spectra of both types of starch after 1 h 15 min ultrasonication is indicative of the severe disruption in the native crystalline structure, namely for waxy maize, and may reflect breakage occurring in the α-1,6 glycosidic linkages.

Based on the above-mentioned results, it may be concluded that the ultrasonic treatment of starch suspensions at low temperature and high sonication power produces significant fragmentation of starch granules, so that they become nano-sized.

3.6. Possible mechanism of generation of SNP

At the frequency used, 24 kHz, the mean diameter of the cavitation bubble is known to be homogeneous around 10–20 μm (Tsochatzidis, Guiraud, Wilhelm, & Delmas, 2001). This diameter is in the same order of magnitude as the size of starch granules, which is around 5–20 μm at the starting point of the ultrasonic treatment. Starch particles should therefore be dragged in the high speed stream resulting from implosion of the cavitation bubbles

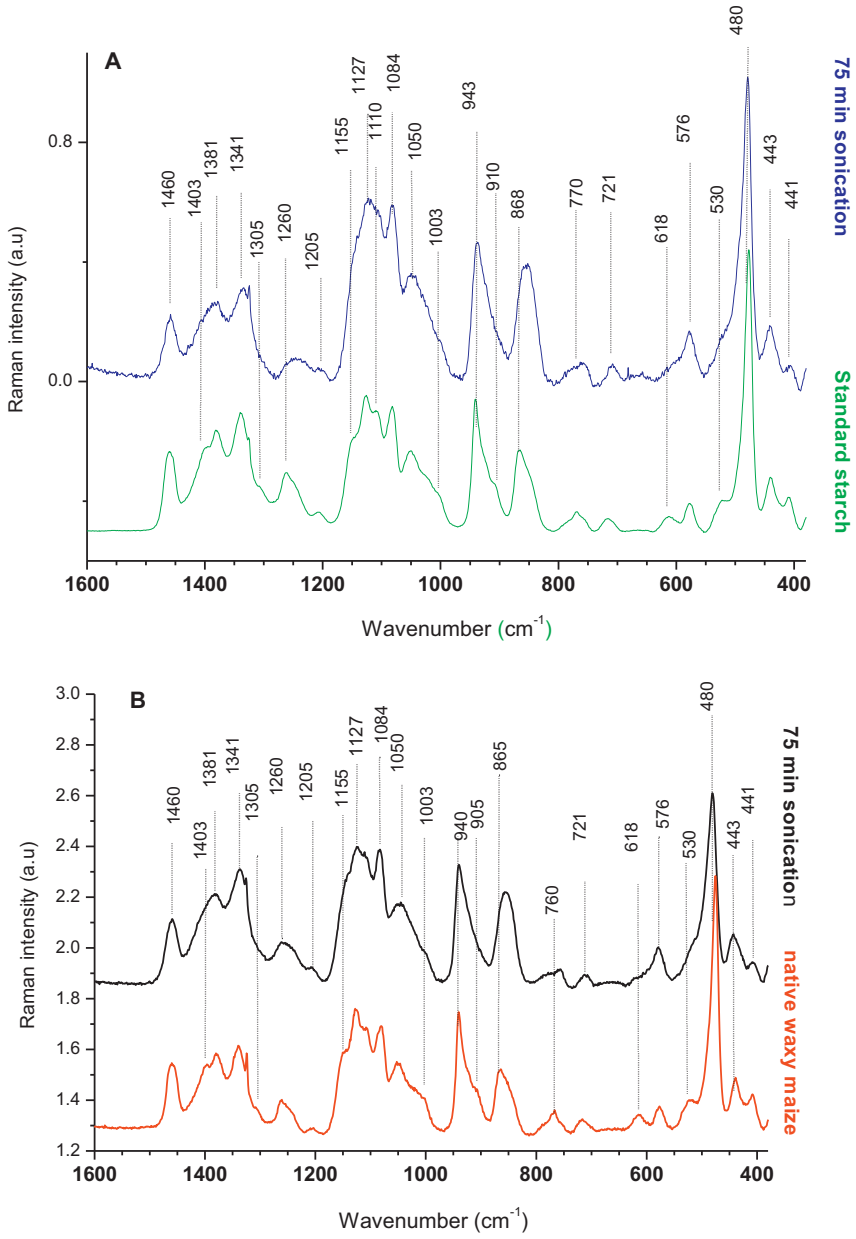

Fig. 7. Raman spectra of (A) standard starch and (B) waxy maize before and after 75 min ultrasound treatment.

rather than experience the direct impact of the microjet rising from collapsing bubbles. In view of the high speed, which is likely to exceed 200 m/s, the starch particles are driven together and collide violently, causing surface damage that leads to a decrease in size (Crum, 1995; Prozorov, Prozorov, & Suslick, 2004) Based on the SEM observations, it is likely that the resulting mechanical collision along with the high shear forces brought about progressive erosion of the starch particles starting from the surface, which underwent further fragmentation until a limiting size was reached. Furthermore, given the low temperature during sonication, water molecules could not diffuse inside the amylopectin chains and no plasticization of the amylopectin phase was likely to take place. Both the amylose and amylopectin chains remained in the glassy domain, encouraging the fragmentation process until the particles became nano-sized, where they could no longer be broken down. The mechanical damage to starch particles under the effect of ultrasonication in an aqueous solution was also highlighted by Yue et al. (2012).

One might invoke the blocklet concept (Gallant, Bouchet, & Baldwin, 1997) in order to explain the formation of SNP under ultrasonication. If we assume that the crystalline and amorphous lamellaes are organized in a discrete asymmetric globular unit named blocklet with a size in the range of 50–100 nm, then the prolonged ultrasonication under temperature of 8–10 °C might bring about the peeling-off of the blocklet and their subsequent break down. However, the blocklet concept is not fully recognized and still a matter of debate. Further investigation and deeper characterization of the ensuing starch nanoparticles using Small Angle X-ray Scattering (SXA), transmission electronic microscopy (TEM) and AFM are ongoing in order to better explain the mechanism of the formation of SNP.

4. Conclusion

An efficient procedure has been described for the preparation of nano-sized starch particles using the purely physical method of

high-intensity ultrasonication without any chemical additives. The process is based on the high power ultrasonication of a suspension of starch granules in water at 1–2% consistency and at a temperature of 8–10 °C, using two types of starch, namely standard maize starch and waxy maize. It was shown that the particle size of the starch granules decreased continuously with the time of ultrasonication treatment to level off after about 75 min to a size ranging from 30 to 140 nm and 30 to 250 nm in the case of standard and waxy maize respectively. Complete conversion of the starch granules from micronic to nanometric scale after 75 min ultrasonication was confirmed by FE-SEM observation, showing clusters of particles ranging in size from 80 to 200 nm. The elementary size of the nanoparticles forming the clusters ranges from 20 to 80 nm. FE-SEM observation at intermediary sonication intervals revealed that with the increasing time of ultrasonication the surface of the granules appeared to be progressively broken down and eroded, with the release of particles 20–100 nm in size. WAXD analysis indicated that sonication seriously disrupts the crystalline structure of clustered amylopectin and seems to lead to nanoparticles with low crystallinity or an amorphous character. Raman analysis confirmed the decrease in crystallinity with ultrasonication treatment and suggests the occurrence of breakage along the branching point formed by the α-1,6 glycosidic linkage.

To the best to our knowledge, this is the first report concerning the preparation of starch-based nanoparticles by high-intensity ultrasonication without any chemical additives. Compared with the acid hydrolysis process, which produces low yields of starch nanocrystals, this process offers the advantage of being quite rapid and easy to implement without the need to undertake repeated washing treatment, since no chemical reagent is added during the process. As no further purification was carried on the suspension of SNP, we infer that the yield of production should be close to 100%.

Acknowledgement

Financial support from PHC UTIQUE (Grant 15G1115) is gratefully acknowledged. The USC "Raman"-University of Sfax-Tunisia is highly acknowledged for Raman measurement.

References

Alila, S., Besbes, I., Rei Vilar, M., Mutjé, P., & Boufi, S. (2013). Non-woody plants as raw materials for production of microfibrillated cellulose (MFC): a comparative study. *Industrial Crops and Products*, *41*, 250–259.

Angellier, H., Molina-Boisseau, S., Lebrun, L., & Dufresne, A. (2005). Processing and structural properties of waxy maize starch nanocrystals reinforced natural rubber. *Macromolecules*, *38*(9), 3783–3792.

Angellier, H., Putaux, J. L., Molina-Boisseau, S., Dupeyre, D., & Dufresne, A. (2005). Starch nanocrystal filler in an acrylic polymer matrix. *Macromolecular Symposia*, *221*, 95–104.

Besbes, I., Rei Vilar, M., & Boufi, S. (2011). Nanofibrillated cellulose from alfa, eucalyptus and pine fibres: preparation, characteristics and reinforcing potential. *Carbohydrate Polymers*, *86*, 1198–1206.

Biskupa, R. C., Rokita, B., Lotfy, S., Ulanski, P., & Rosiak, J. M. (2005). Degradation of chitosan and starch by 360-kHz ultrasound. *Carbohydrate Polymers*, *60*, 175–184.

Chin, S. F., Pang, S. C., & Tay, S. H. (2001). Size controlled synthesis of starch nanoparticles by a simple nanoprecipitation Method. *Carbohydrate Polymers*, *86*, 1817–1819.

Crum, L. A. (1995). Comments on the evolving field of sonochemistry by a cavitation physicist. *Ultrasonics Sonochemistry*, *2*(2), S147–S152.

Degrois, M., Gallant, D. P., Baldo, P., & Guilbot, A. (1974). Effects of ultrasound on starch grains. *Ultrasonics*, *12*, 129–131.

Dufresne, A. (2010). Processing of polymer nanocomposites reinforced with polysaccharide nanocrystals. *Molecules*, *2*(5), 605–611.

Gallant, D. J., Bouchet, B., & Baldwin, P. M. (1997). Microscopy of starch: evidence of a new level of granule organization. *Carbohydrate Polymers*, *32*, 177–191.

Gallant, D., Sterling, C., Guilbot, A., & Degrois, M. (1972). Microscopic effects of ultrasound on structure of potato starch – preliminary study. *Starch/Starke*, *24*, 116–123.

Giezen, F., Jongboom, R., Gotlieb, K., & Boersma, A. (2000). Patent Wo 00/69916.

Izidoro, D. R., Sierakowski, M. R., Haminiuk, C. W. I., De Souza, C. F., & De Paula Scheer, A. (2011). Physical and chemical properties of ultrasonically, spray-dried green banana (*Musa cavendish*) starch. *Journal of Food Engineering*, *104*, 639–648.

Jambrak, A. R., Herceg, Z., Subaric, D., Brncic, J., Brncic, S. R., Bosiljkov, T., et al. (2010). Ultrasound effect on physical properties of corn starch. *Carbohydrate Polymers*, *79*, 91–100.

Jiang, Y., Pétrier, C., & Waite, T. D. (2006). Sonolysis of 4-chlorophenol in aqueous solutions: effects of substrate concentration, aqueous temperature and ultrasonic frequency. *Ultrasonics Sonochemistry*, *13*, 415–422.

Koda, S., Kimura, T., Kondo, H., & Mitone, H. A. (2003). A standard method to calibratesonochemical efficiency of an individual reaction system. *Ultrasonics Sonochemistry*, *10*(3), 149–156.

LeCorre, D., Bras, J., & Dufresne, A. (2010). Starch nanoparticles: a review. *Biomacromolecules*, *11*, 1139–1153.

LeCorre, D., Bras, J., & Dufresne, A. (2011). Ceramic membrane filtration for isolating starch nanocrystals. *Carbohydrate Polymers*, *86*, 1565–1572.

LeCorre, D., Vahanian, E., Dufresne, A., & Bras, J. (2012). Enzymatic pretreatment for preparing starch nanocrystals. *Biomacromolecules*, *13*, 132–137.

Liu, D., Wu, Q., Chen, H., & Chang, P. R. (2009). Transitional properties of starch colloid with particle size reduction from microto nanometer. *Journal of Colloid and Interface Science*, *339*(1), 117–124.

Luo, Z. G., Fu, X. O., He, X. W., Luo, F. X., Gao, Q. Y., & Yu, S. J. (2008). Effect of ultrasonic treatment on the physicochemical properties of maize starches differing in amylose content. *Starch/Starke*, *60*, 646–653.

Mason, T. J., & Lorimer, J. P. (2002). *Applied sonochemistry. The uses of power ultrasound in chemistry and processes*. Weinheim: Wiley-VCH Verlag GmbH.

Moon, R. J., Martini, A., Nairn, J., Simonsen, J., & Youngblood, J. (2011). Cellulose nanomaterials review: structure, properties and nanocomposites. *Chemical Society Reviews*, *40*, 3941–3994.

Mutungi, C., Passauer, L., Onyango, C., Jaros, D., & Rohm, H. (2012). Debranched cassava starch crystallinity determination by Raman spectroscopy: Correlation of features in Raman spectra with X-ray diffraction and ^{13}C CP/MAS NMR spectroscopy. *Carbohydrate Polymers*, *87*, 598–606.

Prozorov, T., Prozorov, R., & Suslick, K. S. (2004). High velocity interparticle collisions driven by ultrasound. *Journal of the American Chemical Society*, *126*(43), 13890–13891.

Putaux, J. L., Molina-Boisseau, S., Momaur, T., & Dufresne, A. (2003). Platelet nanocrystals resulting from the acid hydrolysis of waxy maize starch granules. *Biomacromolecules*, *4*(5), 1198–1202.

Siqueira, G., Bras, J., & Dufresne, A. (2010). Cellulosic bionanocomposites: a review of preparation, properties and applications. *Polymers*, *2*, 728–765.

Siró, I., & Plackett, D. (2010). Microfibrillated cellulose and new nanocomposite materials: a review. *Cellulose*, *17*, 459–494.

Song, D., Thioc, Y. S., & Deng, Y. (2011). Starch nanoparticle formation via reactive extrusion and related mechanism study. *Carbohydrate Polymers*, *85*, 208–214.

Tester, R. F., Karkalas, J., & Qi, X. (2004). Starch – composition, fine structure and architecture. *The Journal of Cereal Science*, *39*, 151–165.

Tome, L. C., Pinto, R. J. B., Trovatti, E., Freire, C. S. R., Silvestre, A. J. D., Pascoal Neto, C., et al. (2011). The irruption of polymers from renewable resources on the scene of macromolecular science and technology. *Green Chemistry*, *13*, 1061–1083.

Tsochatzidis, N. A., Guiraud, P., Wilhelm, A. M., & Delmas, H. (2001). Determination of velocity, size and concentration of ultrasonic cavitation bubbles by the phase-Doppler technique. *Chemical Engineering Science*, *56*, 1831–1840.

Wildi, R. H., Van Egdob, E., & Bloembergen, S. Patent US2011/0042841 A1.

Yue, Y., Zuo, J., Hébraud, P., Hemar, Y., & Ashokkumar, M. (2012). Quantification of high-power ultrasound induced damage on potato starch granules using light microscopy. *Ultrasonics Sonochemistry*, *19*, 421–426.

Zeng, J. B., He, Y. S., Li, S. L., & Wang, Y. Z. (2012). *Chitin Whiskers: An Overview Biomacromolecules*, *13*(1), 1–11.

Zhbankov, R. G., Andrianov, V. M., & Marchewka, M. K. (1997). Fourier transform IR and Raman spectroscopy and structure of carbohydrates. *Journal of Molecular Structure*, 436–437.

Zhu, J., Li, L., Chen, L., & Li, X. (2012). Study on supramolecular structural changes of ultrasonic treated potato starch granules. *Food Hydrocolloids*, *29*, 116–122.

Zobel, H. F. (1964). X-ray analysis of starch granules. In L. R. Whistler, & R. J. Smith (Eds.), *Methods in carbohydrate chemistry* (pp. 109–113). New York: Academic press.